

WESTINGHOUSE CFD MODELING AND RESULTS FOR EPRI NESTOR CFD ROUND ROBIN EXERCISE OF PWR ROD BUNDLE TESTING

M. E. Conner and Z. E. Karoutas

Westinghouse Electric Company
Hopkins, SC, USA

connerme@westinghouse.com; karoutze@westinghouse.com

Y. Xu

Westinghouse Electric Company
Cranberry Township, PA, USA

xuy@westinghouse.com

ABSTRACT

This paper presents the CFD modeling and results of Westinghouse Electric Company obtained as part of the EPRI NESTOR CFD Round Robin Exercise. NESTOR, which stands for New Experimental Studies of Thermal Hydraulics of Rod Bundles, was a joint CEA-EDF-EPRI project in which high fidelity thermal hydraulic data was obtained in PWR test bundles at test conditions including actual PWR conditions. Westinghouse participated in the entire Round Robin Exercise, and modeled both the Phase 1 (Simple Support Grid rod bundle tests) and the Phase 2 (Mixing Vane Grid rod bundle tests) problems. This paper presents the Westinghouse results and insights gained from this EPRI program.

STAR-CCM+ was used for all CFD models. There were four basic test problems that were modeled. Test data was provided to the participants for comparison. Different turbulence models were used based on the problem. Sensitivity studies were performed on mesh and turbulence models. Comparison of CFD results and test data are shown, and conclusions on how best to model these PWR configurations are provided.

Westinghouse has performed extensive CFD modeling of PWR rod bundles under normal operating conditions. Experience from these prior CFD models, as well as experience gained as part of this round robin exercise, is used to support conclusions made by Westinghouse for input to the Best Practice Guidelines that all Round Robin participants are contributing too.

KEYWORDS

PWR, Fuel Assembly, Mixing Vane Grid, CFD, EPRI, NESTOR

1. INTRODUCTION

In January 2011, EPRI (Electric Power Research Institute) sent out invitations to participate in a round robin CFD benchmark exercise for PWR applications. The objective of the exercise is to develop best practice guidance for CFD users that can be applied to future PWR assembly and core designs. Westinghouse (Westinghouse Electric Company) chose to participate in this EPRI program to learn from other participants and to contribute to the Best Practice Guidelines that will be the end result of this collaborative round robin exercise. The key participants of this EPRI program are ANSYS, AREVA, CD-adapco, CEA, EDF, EPRI, Texas A&M University, and Westinghouse [1].

Benchmark experimental data used in this CFD round robin exercise is taken from the NESTOR testing program. NESTOR (New Experimental Studies of Thermal-Hydraulics of Rod Bundles) was a joint CEA-EDF-EPRI collaborative experimental program that tested simple support grid (SSG) and mixing vane grid (MVG) designs for PWR fuel bundles in the 2005-2009 timeframe [2]. NESTOR provided high fidelity thermal hydraulic data, including unique temperature data that was obtained at actual PWR operating conditions.

This EPRI CFD round robin exercise was broken into Phase 1 (SSG rod bundle tests) and Phase 2 (MVG rod bundle tests) problems. The SSG grid design was designed to impact the flow field as little as possible, while mechanically supporting the test rods and maintaining the appropriate fuel rod pitch. Figure 1 shows the SSG grid used in the NESTOR testing. The MVG design used in the NESTOR testing is a 5x5 test grid of the Westinghouse 17x17 V5H midgrid design. This MVG utilizes a split style mixing vane pair at the strap intersections to promote mixing and lateral flow structures to improve the thermal performance of the fuel design. Figure 2 provides a picture of an actual MVG test grid.

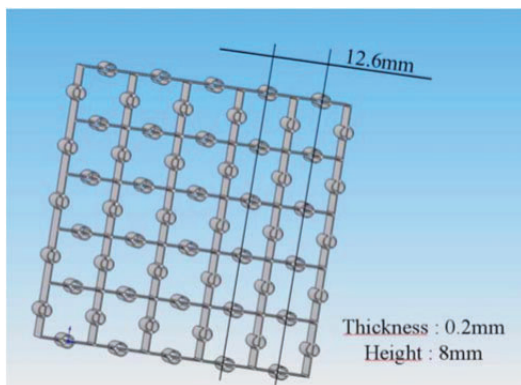


Figure 1. SSG Grid used in NESTOR Testing.
(figure taken from [2])

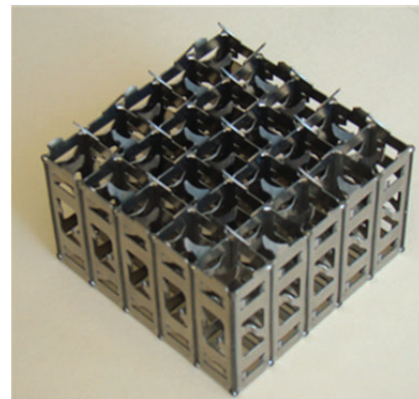


Figure 2: MVG Grid used in NESTOR Testing.
(picture of actual test grid)

1.1. Westinghouse CFD Methodology Development

Since the mid-90's, Westinghouse has extensive experience using CFD to analyze flow and heat transfer in PWR rod bundles. Benchmark experimental data is key to developing a CFD modeling methodology. To obtain benchmark data, Westinghouse has had long term collaborations with universities in the United States: Clemson University from 1995-2005 [3-6], and Texas A&M University from 2009 to the present [7-8].

Previously, Westinghouse developed a CFD methodology for single-phase flow in PWR fuel assemblies [9] utilizing the STAR-CD CFD code. From that development effort, it was concluded that a successful CFD methodology requires benchmarking of the combined effects of the domain, mesh, solver, and turbulence model. Utilizing this methodology, Westinghouse has successfully utilized CFD in determining the root-cause for in-core localized crud issues, in analyzing core designs to avoid crud issues, and developing a new mixing vane design.

Westinghouse is now moving to the STAR-CCM+ CFD code for PWR fuel analyses. To develop the methodology for STAR-CCM+, this same approach is being used. In this case, the availability of the

NESTOR test data from the EPRI round robin exercise provides excellent benchmark data at PWR conditions that was used to establish the domain, mesh, solver, and turbulence model to be used in STAR-CCM+ for PWR analyses.

2. TEST DATA

The NESTOR test program utilized two different test bundle geometries and two different test facilities. The test bundles differed by the type of structural grids used. Two test facilities were used to measure different test data at different conditions. The first test facility - the EDF MANIVEL loop in Chatou, France - was used to measure axial velocities in the rod bundle and pressure drop across the test grids in an isothermal test. The second test facility - the CEA OMEGA loop in Grenoble, France - was used to measure rod temperatures and end of bundle fluid temperatures in a thermal test at PWR conditions. Additional details regarding the test data can be found in [1].

2.1. Rod Bundle Geometry

Axial rod bundles representative of 17x17 PWR fuel assemblies were used in this testing, and in the subsequent CFD simulations. The array size used in this testing is 5x5, with all 25 rods representing actual fuel rods with an outer diameter of 9.5 mm (0.374 inch) on a 12.6 mm (0.496 inch) rod pitch. The inner wall dimension of the test housing for both the MANIVEL and OMEGA tests is 66.1 mm (2.60 inch). The axial length of the OMEGA test bundle is greater than 3658 mm (12 feet) to accommodate a total heated length for OMEGA testing of 3.658 m (12 feet). The MANIVEL test bundle is also greater than 3658 mm (12 feet) to ensure that the OMEGA flow field is consistent with the OMEGA flow field. Figures showing the axial test bundle geometries can be found in [1].

The OMEGA test rods are made out of Inconel 600 and are electrically heated to produce heat fluxes that are prototypical of PWR rod powers. The rods are hollow, and a special instrumentation fixture was developed to measure the rod inner diameter temperature using two discrete thermocouples. The entire thermocouple fixture can be rotated to measure azimuthal temperatures around the entire inner circumference of the rod. Additionally, the fixture can be moved axially to measure temperatures at difference axial elevations.

2.2. SSG Testing

The first test assembly was the SSG bundle, and it used only the SSG grids shown in Figure 1. The SSG grids were spaced on approximately a 279 mm (11 inch) grid span. As noted in Section 1, the purpose of the SSG grid design was to support the test rods on the appropriate rod pitch while disturbing the flow field as little as possible.

From MANIVEL testing, the axial fluid velocity was measured along horizontal lines at various axial locations. The data at select locations is plotted with the CFD predictions in Section 3. Another measurement that was taken was the pressure drop across the test grids. This data can be compared to CFD predictions as well.

From OMEGA testing, predicted CFD rod ID temperatures can be compared against test data. This can be done by either comparing the average temperature at a given elevation or by comparing the azimuthal temperature distribution. Additionally, the end of heated length fluid temperatures can be compared to CFD predictions field.

2.3. MVG Testing

The second test assembly was the MVG bundle, and the MVG's (shown in Figure 2) were placed on a 558 mm (22 inch) grid span. Due to the electrical Gaussian forces in the OMEGA test, SSG grids are used midway between MVG's to prevent bowing of the test rods in the OMEGA testing. To mimic this geometry in MANIVAL, SSG's are also used in the MANIVEL testing.

MANIVEL and OMEGA test data as described above for the SSG bundle was also acquired from the MVG bundle.

2.4. Test Conditions

The test conditions for the four tests that are compared to CFD results in this paper are provided in Table I for MANIVEL testing and Table II for OMEGA testing. As can be seen in these tables, the test conditions between SSG and MVG testing are very similar.

Table I. MANIVEL Test Conditions

MANIVEL Test	Outlet Pressure, P (bar)	Flow Rate, Q (m ³ /h)	Outlet Temperature, T (°C)
SSG Bundle	1	60.7	30.4
MVG Bundle	1	64.7	29.7

Table II. OMEGA Test Conditions

OMEGA Test	Outlet Pressure, P (bar)	Flow Rate, Q (m ³ /h)	Inlet Temp, T (°C)	Total Heating Power (kW)	Hot Rod Power (kW)	Heat Flux (W/m ²) [Btu/hr-ft ²]
SSG Bundle	156	3560	271.2	2037	94.81	868,400 [275,500]
MVG Bundle	155.7	3520	271.1	2041	95.46	874,400 [277,400]

3. CFD MODELING

CFD benchmarking activities were divided into two phases distinguished by the grid design(s) used in the test bundle. SSG grids were tested in Phase 1; while Phase 2 focused on the MVG grids. Each phase consisted on modeling one MANIVEL test and one OMEGA test. The test conditions are defined above in Tables I and II. The focus of this paper is on the MVG test and CFD models, however some SSG CFD results will be presented.

All CFD models were built in STAR-CCM+ V7.06.012, including meshing, physical modeling, numerical solving and result post-processing. A simulation was stopped manually when it was judged converged based on the stability (no changed or slight oscillation around a constant value over hundreds of iterations) of monitored residuals (continuity, momentum, energy) and variables (such as turbulent kinetic energy, vorticity, axial velocity, cross-section averaged pressure).

3.1. Phase 1 (SSG) Modeling and Results

A CFD model of one span (279 mm) of the MANIVEL-SSG test section was built with trim mesher. A steady state simulation was conducted with $k-\epsilon$ Realizable turbulence model and two layer all y^+ wall treatments. Good agreement is obtained from a typical comparison between the CFD results and the test data. An example of the axial velocity at an elevation of $z=35$ mm downstream of the SSG grid is shown in Figure 3. The “slices” shown in Figure 3 represent horizontal lines through the cross-sectional flow field that pass through the centerline of the subchannel centers.

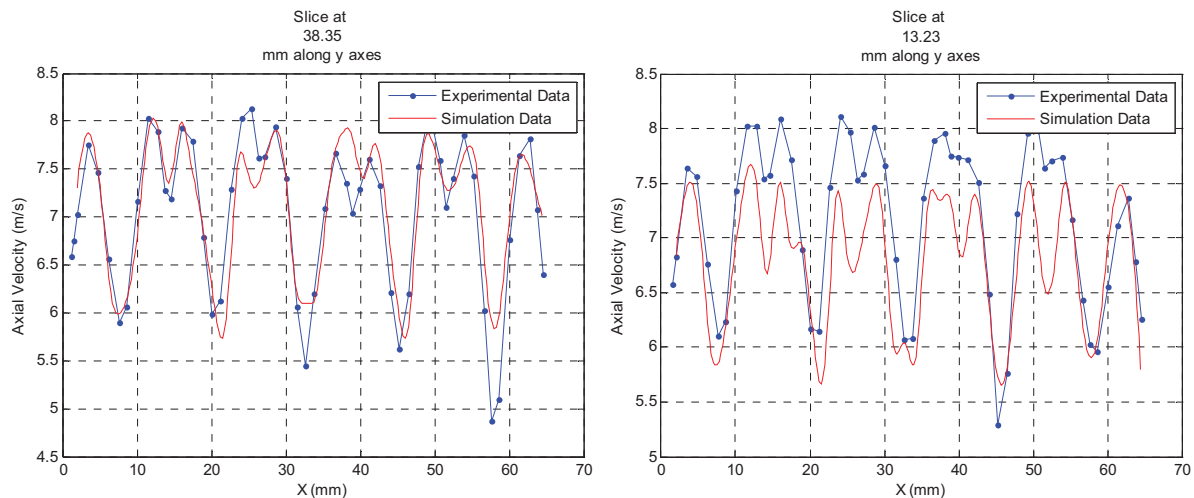


Figure 3. Comparison of CFD and Test Data from SSG-MANIVEL Test.

In building the OMEGA-SSG CFD model, a single span model was created first and then this single span was copied to create the whole domain. A steady state simulation was conducted with standard $k-\epsilon$ low Reynolds number turbulence model and all y^+ wall treatments. Sensitivity study was investigated with two meshes and four turbulence models (standard $k-\epsilon$ low Reynolds number, $k-\epsilon$ Realizable, $k-\omega$, standard $k-\epsilon$ cubic relation between Reynolds stress and strain rate tensor). The CFD model with the low Reynolds number $k-\epsilon$ turbulence model and $y^+=1$ mesh gives the closest rod surface temperature to the experimental value as shown in Figure 4, which is taken at an elevation far downstream of the SSG grid.

3.2. Phase 2 (MVG) Modeling and Results

In Phase 2, CFD modeling was primarily focused on mixing vane grids effects on fluid flow (MANIVEL-MVG) and heat transfer (OMEGA-MVG). Therefore, the results downstream of the SSG grids that are in the MVG test bundle are not the focus here. The MANIVEL-MVG data was used to benchmark turbulence models and mesh strategies in terms of velocity profiles. The OMEGA-MVG data was used to benchmark the rod surface and coolant temperatures. Simplifications in the MVG model utilized in the CFD models are described in Section 3.3.

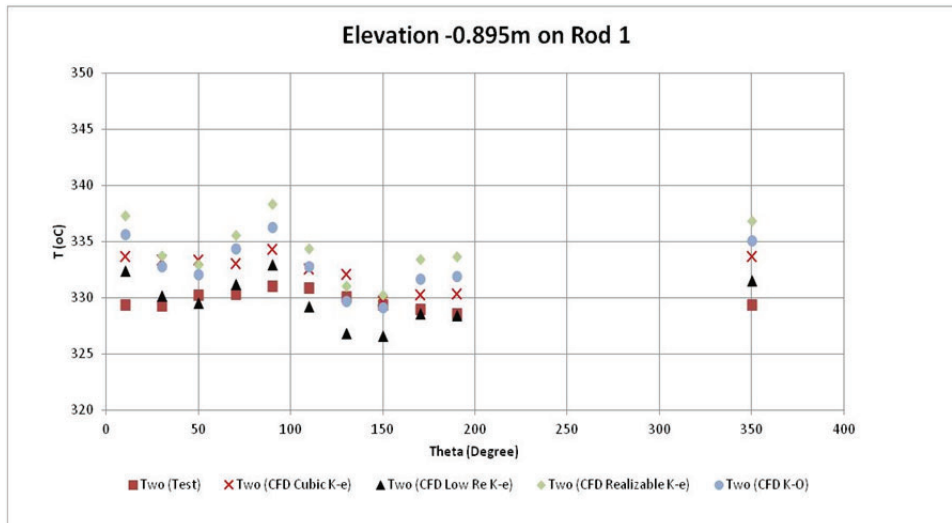


Figure 4. Comparison of Azimuthal Rod Surface Temperature Results from CFD versus Test Data from OMEGA-SSG Test.

3.2.1. MANIVEL-MVG

The CFD domain for the MANIVEL-MVG case includes 2 MVGs and 4 SSGs, on an approximate 279 mm grid span (between SSG and MVG, or between the final two SSGs). This includes a SSG grid and associated rod bundle region below the first MVG, a SSG grid midway between the 2 MVGs, and 2 SSG grids downstream of the second MVG. Extra lengths were included at the inlet and the outlet of the model for the purpose of avoiding boundary effects to the simulations. The total mesh cells were from 20 to 100 million depending on mesh refinement options (a typical mesh was about 50 million cells).

Several mesh refinement options were practiced. The effects of mesh density and prism layer refinements are straightforward and easy to understand. Axially scaled is an approach of reducing the axial geometric length by a scaling factor (4 in this analysis), meshing it and then expanding the mesh with the same scaling factor. The wake region refinement is the option of changing the base size in one or all of the directions in the region behind pre-selected structure boundaries (MVGs in this case). Figure 5 shows typical meshes in mesh refinements of scaled and wake approaches. The axial mesh size is clearly larger in the scaled mesh (Figure 5b) than it is without it (Figure 5a). It can be seen that the mesh size was reduced after the MVGs in Figure 5d. A drawback for wake region refinement is that the mesh cells are not refined where the selected boundaries are absent even though the cells are just next to a selected boundary.

Calculated span pressure drop from the CFD simulation was compared against the test data. For the mixing vane grid, the pressure drop was predicted very well (2% high versus measured). For the SSG, the pressure drop in the CFD simulation was about 10% low versus the measure test data.

The axial velocity and axial velocity root-mean-square values of the CFD simulations were plotted against the test data. For page limitation concerns, the plots are not attached to this paper. In general, CFD models predict flow fields reasonably well in fuel assembly bundles. The following key points are concluded from these CFD models:

1. Axially scaled meshing is an efficient approach of saving mesh cells in the dominant flow direction. Scaling up to four times was evaluated in the current application. However, an appropriate scaling factor may be dependent of geometry complexity and flow situations.
2. Base size of 0.5 mm is sufficient for fuel assembly applications.
3. For this isothermal analysis, more prism layers (up to 25 prism layers) and use of the two-layer all y^+ wall treatment is better. However, improvement is not significant considering substantial increase of computing cost. Therefore, high y^+ near wall prism layer meshing is appropriate for rod bundle simulations.
4. Wake region refinement does not improve simulation accuracy proportional to cell counts. Optimal settings may be helpful of improving its performance.
5. Among the selected three turbulence models, $k-\omega$ SST model over-predicts the peak values of axial velocity even though a refined prism layer mesh was used comparing to $k-\varepsilon$ Realizable and Standard $k-\varepsilon$ Quadratic models. The performance difference between the two $k-\varepsilon$ turbulence models is very small. It is insufficient to judge these two models based on flow fields only. Thermal data may be useful in this aspect.

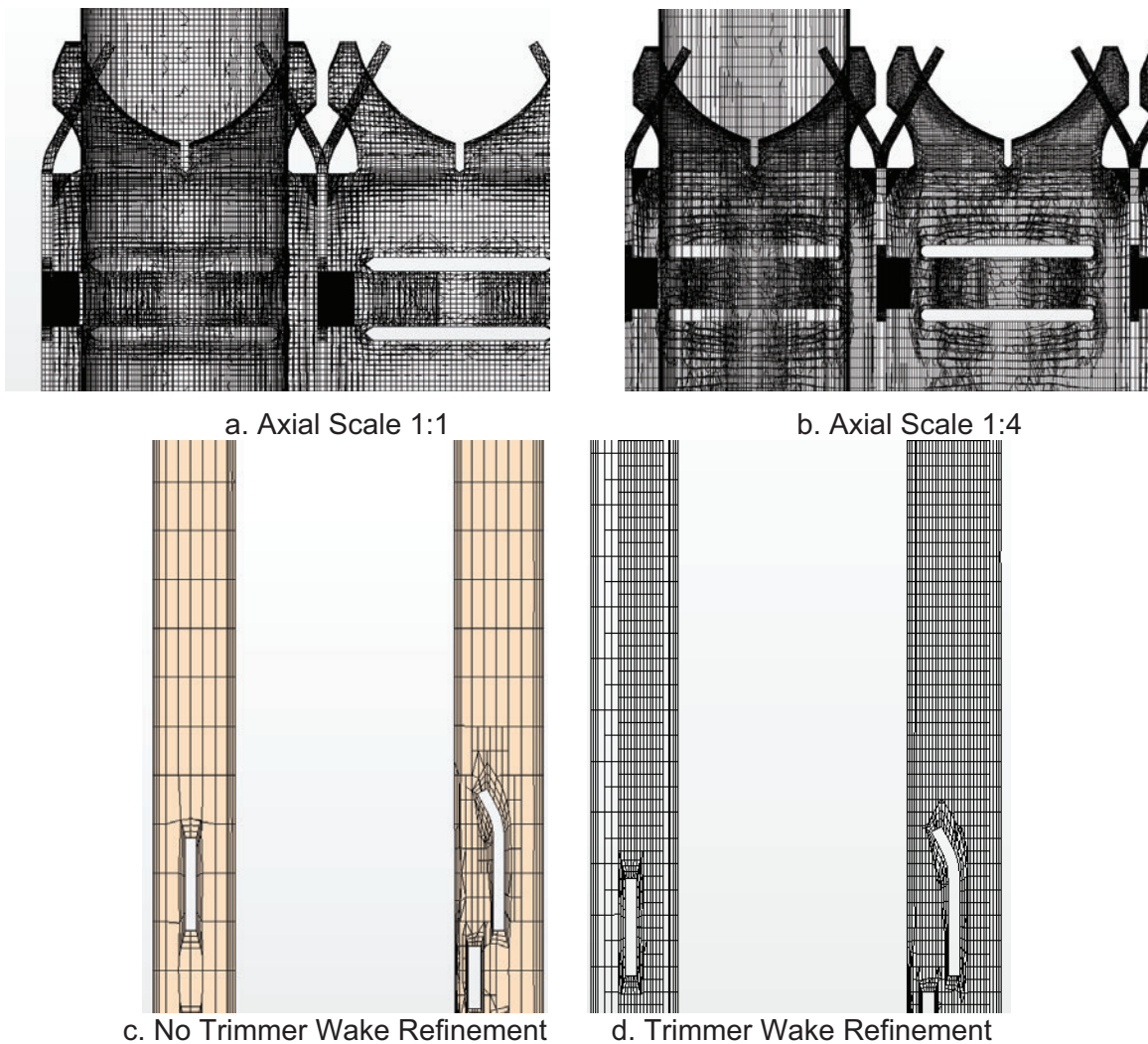


Figure 5. Typical MANIVEL-MVG Meshes for Different Mesh Strategies.

3.2.2. OMEGA-MVG

The OMEGA-MVG CFD domain included all of MVG and SSG grids in the heated length of the test bundle. Some extra length was added to the end of heated length to avoid boundary effects on numerical solutions. The fluid region was meshed with trim mesher; while the solid regions, including rod cladding and grids, were meshed with thin mesher. Three prism layers were generated near wall boundaries in the fluid region. Five thin layers and two prism layers (one for each face) were created, providing high enough thermal gradients in the solid regions. Cell count is typically about 150 million.

Figure 6 shows the typical views of meshes in the axial direction (a) and prism layers (b). Figure 6a shows the mesh mapped on the solid and coolant interface of the rods. The polygons are due to the polygonal prisms for polyhedral cell type in the thin mesher and the rectangles are generated from trim meshing, creating a non-conformal boundary. Longer mesh length along the axial direction is due to geometry scaling operations before and after meshing. The small geometries, such as the thicknesses of cladding and spacer grids were well resolved with thin meshing. Mesh density inside the solids is higher than in the fluid, especially in the radial direction due to thin mesh setting. This is desirable since high radial temperature gradients are expected along solid thickness direction. The cell dimensions at both sides of the interface between fluid and solid regions are very close.

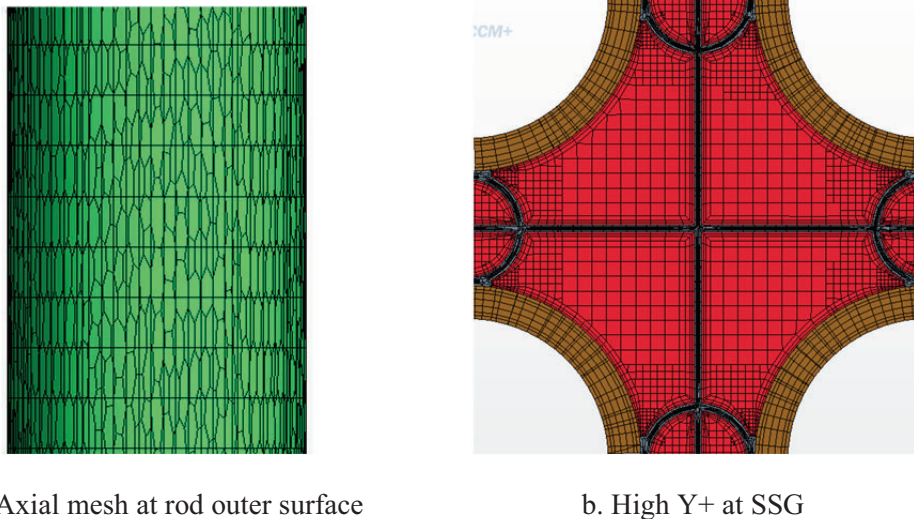


Figure 6. Typical OMEGA-MVG Meshes.

Based on experience gained from SSG benchmarking of Phase 1 and MANIVEL-MVG benchmarking of Phase 2, major physical and numerical settings for RANS approach were chosen as follows:

- Turbulence model: Standard k- ϵ with quadratic relation between Reynolds stress and strain rate tensor, and wall treatments of two-layer all Y+ (applicable to high Y+ mesh),
- Conjugate heat transfer: In-place interfaces,
- Steady State and Segregated AMG linear flow and temperature solvers,
- 2nd order numerical discretization scheme.

In the OMEGA-MVG tests, cladding inner surface temperatures were measured at multiple elevations for the inner nine rods. Sub-channel coolant temperatures were measured at the EOHL indicating thermal

mixing. The inner surface temperatures of the center rod (Rod 5) and a rod diagonal from the center rod (Rod 1) are presented. Figure 7 shows the inner surface temperatures at three elevations.

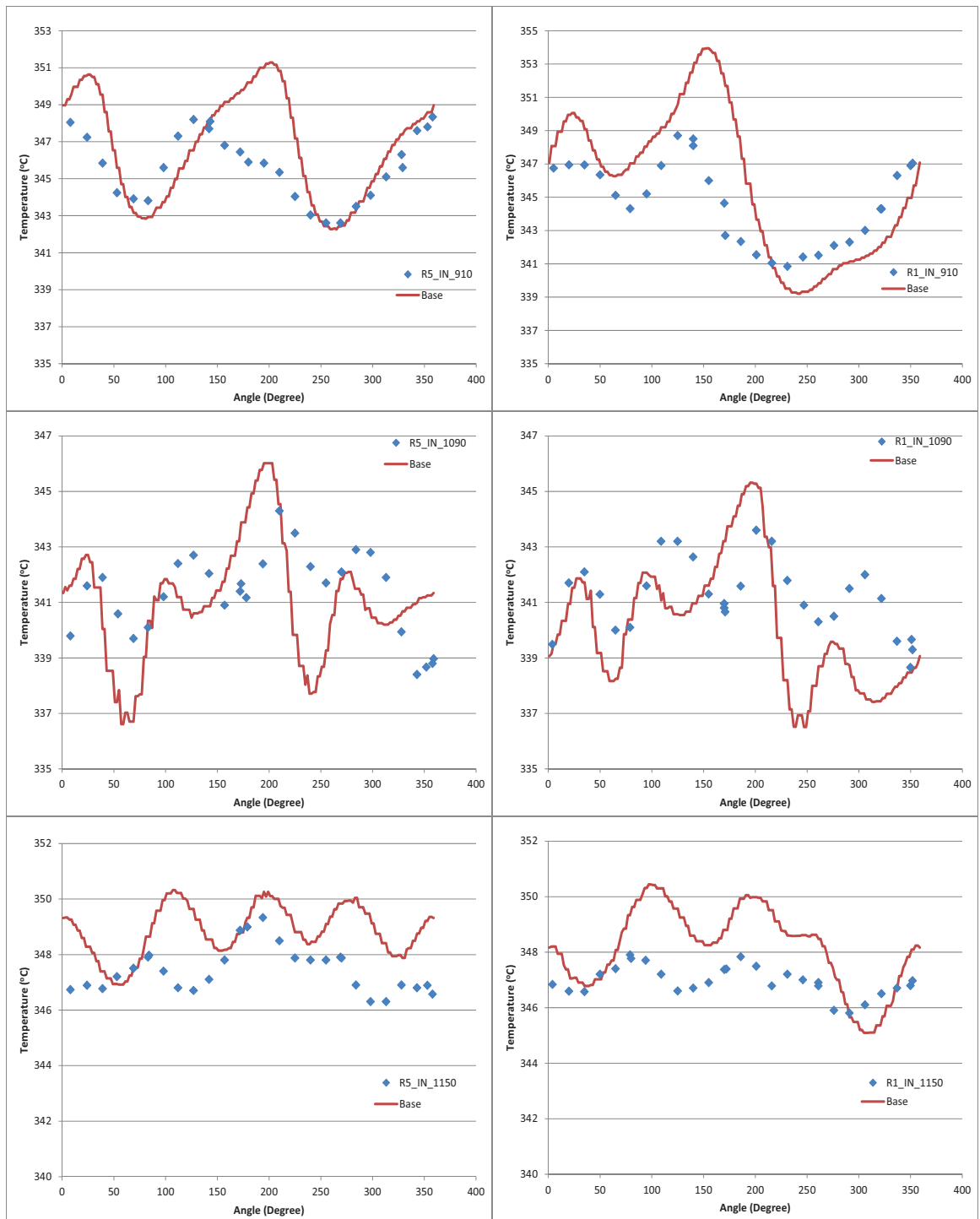


Figure 7. Inner Surface Temperatures of Rod 5 (Center Rod) and Rod 1.

From Figure 7, typical effects of MVG on surface temperatures can be observed:

1. Test Elevation = -910 mm: far downstream (200 mm) of a MVG (but upstream of a SSG)
 - At this elevation, the mixing flow created by the mixing vanes is mostly dissipated. Accordingly, the temperature distribution is dominated by the axial flow. Temperature differences in shape between Rod 5 and Rod 1 are probably due to the orientations of the mixing vanes and the radial power shape. The CFD model correctly predicts these differences.

2. Test Elevation = -1090 mm: just downstream (18 mm) of a MVG
 - At this elevation, the temperature distribution was disturbed by the mixing flow produced by the mixing vanes on the top of the MVG. Due to flow separation or vortex shedding from the solids, such as straps and vanes, flow prediction is most difficult in this area. Correspondingly, large differences of both shape and peak values between the CFD results and the data were observed. Interestingly, the averaged values are well predicted on both rods.

3. Test Elevation = -1150 mm: just upstream of a MVG
 - At this elevation, mixing flow has become very small. Rod temperature is inversely proportional to coolant inventory: i.e. the narrow rod gaps are expected to have the highest temperatures. The CFD model over-predicts the rod surface temperatures.

The test data and the CFD results of the coolant temperature at the EOHL are compared in Figure 8. In general, agreement is reasonable, though noticeable differences occur at some of sub-channels. To better view where the large differences occur, the temperature differences in percentage between the test data and CFD results are tabulated in Figure 8. The four empty sub-channels are due to unavailability of the test data. It can be seen that most of the large differences occur at either the corner or side sub-channels.

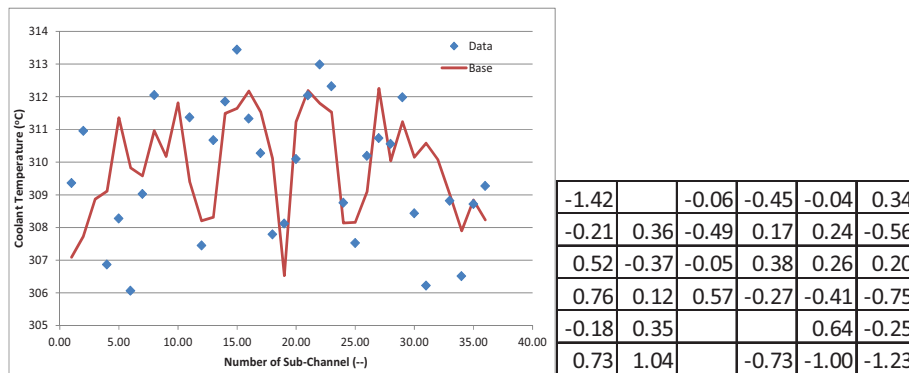


Figure 8. Sub-Channel Coolant Temperature at EOHL for CFD (“Base”) versus Test Data.

3.3. Simplifications of MVG for CFD Modeling

To reduce the number of CFD cells required to model the MVG details, simplifications are used in the solid model of the MVG design. Westinghouse has extensive experience with the following simplifications demonstrating that these have negligible impact on the results of the CFD simulation.

1. Spring or Dimple to Rod Contact – As manufactured, the interface between a rod support feature (i.e., a spring or a dimple) and the fuel rod is typically a line contact. The very small gaps between the rod support feature and the fuel rod near the line contact have very little flow, but require a large number of cells to model with acceptable shapes. Therefore, in the solid model, blocks are added to the rod contact region of the springs and dimples to form a wider contact with the rods. This simplifies meshing these regions and has negligible effect on the flow field downstream of the mixing vanes.
2. Weld Nuggets – As manufactured, weld nuggets have a complex shape. To simplify the meshing of the region around the weld nuggets, a simplified geometric shape, such as a cone with a square base, is used. This assumed weld nugget shape provides the appropriate blocked area and approximate shape, and has been shown to have negligible impact on the flow field downstream of the mixing vanes.
3. Vertical Grid Strap Slots – As manufactured, these are numerous vertical slots at strap intersections to allow assembly of the grid straps together. These vertical slots have essentially no impact on the flow downstream of the mixing vanes and are therefore, removed from the MVG solid model by filling them in.
4. Other features that are small and not in the axial flow field can be removed from the solid model to avoid wasting mesh to model them correctly.

4. CONCLUSIONS

The NESTOR experimental test data provides a unique set of outstanding benchmark data for PWR rod bundles. Especially unique from NESTOR is the heat transfer data at the inner diameter of heater rods at PWR conditions.

The CFD modeling performed by Westinghouse and provided in this paper utilizes steady-state RANS calculations. Therefore, this CFD method will never predict the NESTOR experiment exactly. However, reasonable results are achievable, as has been shown in this paper. While STAR-CCM+ was utilized in the CFD calculations shown in this paper, it is not required to use this CFD code to get reasonable results. A successful CFD methodology requires benchmarking of the combined effects of the domain, mesh, solver, and turbulence model.

NOMENCLATURE (IF NEEDED)

CEA	Commissariat à L’Energie Atomique et aux Energies Alternatives
CFD	Computational Fluid Dynamics
CHT	conjugate heat transfer
D	hydraulic diameter
EDF	Électricité de France
EOHL	end of heated length
EPRI	Electric Power Research Institute
L/D	axial length to hydraulic diameter ratio
LDV	Laser Doppler Velocimetry

MANIVEL	EDF hydraulic test loop in Chatou, France
MVG	mixing vane grid
NESTOR	New Experimental Studies of Thermal-Hydraulics of Rod Bundles
OMEGA	CEA thermal-hydraulic test loop in Grenoble, France
PWR	Pressurized Water Reactor
SSG	simple support grid

ACKNOWLEDGMENTS

We would like to acknowledge the other participants of the Round Robin Exercise from which this work originated. A truly collaborative effort was accomplished by the key participants: ANSYS, AREVA, CD-adapco, CEA, EDF, EPRI, and Texas A&M University. We have enjoyed working with our colleagues from these entities over the past 4 years, and look forward to continued collaboration.

REFERENCES

1. D. M. Wells, P. Peturaud, S. K. Yagnik, "Overview of CFD Round Robin Benchmark of the High Fidelity Fuel Rod Bundle NESTOR Experimental Data," *Proceedings of the 16th International Topical Meeting on Nuclear Reactor Thermal Hydraulics (NURETH-16)*, Chicago, Illinois, USA, August 30 – September 4, 2015 (2015).
2. A. Bergeron, T. Chataing, E. Décossin, J. Garnier, P. Péturaud, S. K. Yagnik, "Design, Feasibility, and Testing of Instrumented Rod Bundles to Improve Heat Transfer Knowledge in PWR Fuel Assemblies," *Proceedings of the 2007 International LWR Fuel Performance Meeting*, San Francisco, California, USA, September 30 – October 3, 2007 (2007).
3. H. L. McClusky, M. V. Holloway, T. A. Conover, D. E. Beasley, M. E. Conner, and L. D. Smith, III, "Mapping of the Lateral Flow Field in Typical Subchannels of a Support Grid with Vanes," *ASME Journal of Fluids Engineering*, **Vol. 125**, 987-996 (2003).
4. M. V. Holloway, H. L. McClusky, D. E. Beasley, and M. E. Conner, "The Effect of Support Grid Features on Local, Single-Phase Heat Transfer Measurements in Rod Bundles," *ASME Journal of Heat Transfer*, **Vol. 126**, 43-53 (2004).
5. M. V. Holloway, T. A. Conover, H. L. McClusky, D. E. Beasley, and M. E. Conner, "The Effect of Support Grid Design on Azimuthal Variation in Heat Transfer Coefficient for Rod Bundles," *ASME Journal of Heat Transfer*, **Vol. 127**, 598-605 (2005).
6. M. V. Holloway, D. E. Beasley, and M. E. Conner, "Single-phase Convective Heat Transfer in Rod Bundles," *Nuclear Engineering and Design*, **Vol. 238**, 848-858 (2008).
7. M. E. Conner, E. E. Dominguez-Ontiveros, and Y. A. Hassan, "Hydraulic Benchmark Data for PWR Mixing Vane Grid," *Proceedings of the 14th International Topical Meeting on Nuclear Reactor Thermal-Hydraulics (NURETH-14)*, Toronto, Canada, September 25-29, 2011 (2011).
8. M. E. Conner, E. E. Dominguez-Ontiveros and Y. Hassan, "Advanced Hydraulic Benchmark Data for PWR Mixing Vane Grid," *Proceedings of the 15th International Meeting on Nuclear Reactor Thermalhydraulics NURETH-15*, Pisa Italy, May 12-15, 2013 (2013).
9. M. E. Conner, E. Baglietto, A. M. Elmahdi, "CFD Methodology and Validation for Single-Phase Flow in PWR Fuel Assemblies," *Nuclear Engineering and Design*, journal topical issue, Experiments and CFD Code Applications to Nuclear Reactor Safety (XCFD4NRS), **Volume 240** (9), September 2010 (2010).